# Cation-Stacking Approach Enabling Interconversion between Bis(xanthylium) and Its Reduced Species

Moto Kikuchi,[a] Tomoki Tadokoro,[a] Takuya Tachibana,[a] Shuichi Suzuki,[b] Takanori Suzuki[a] and Yusuke Ishigaki*[a]

[a] Department of Chemistry, Faculty of Science, Hokkaido University, Sapporo, Hokkaido 060-0810, Japan

[b] Graduate School of Engineering Science, Osaka University, Toyonaka, Osaka 560-8531, Japan

Correspondence to: yishigaki@sci.hokudai.ac.jp (Y.I.)

**Graphical Abstract:**

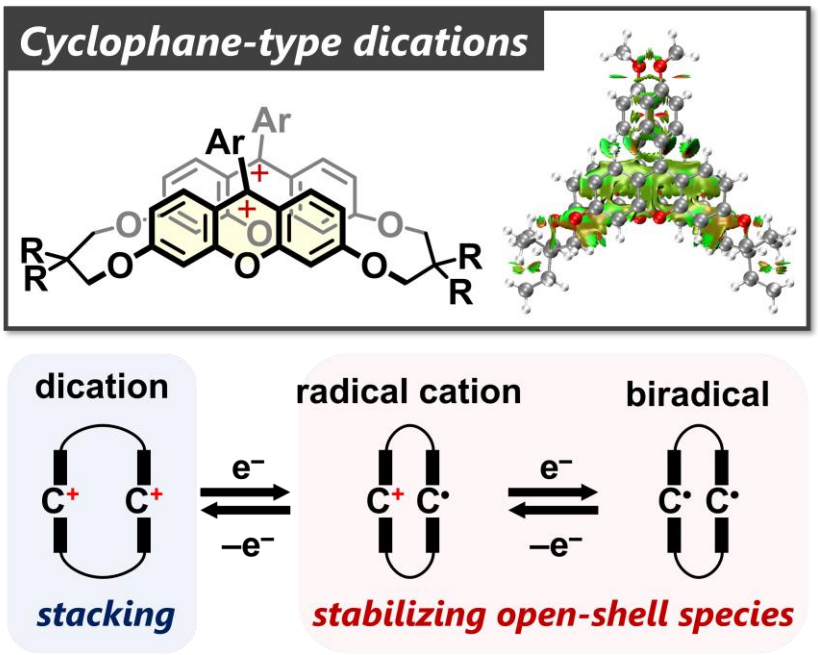


**Abstract:** Cyclophane-type dications with two units of xanthylium were designed, with the expectation that intramolecular interaction between cation units could induce changes in absorption and redox behavior. The desired dications were synthesized via the macrocyclic diketone as a key intermediate, which was efficiently obtained by a stepwise etherification. X-ray and UV/Vis measurements revealed that the cyclophane-type dications adopt a stacking structure in both the crystal and solution. Due to the intramolecular interaction caused by π-π stacking of the xanthylium units, a considerable blue shift compared to the corresponding monocations and a two-stage one-electron reduction process were observed in the dications. Furthermore, upon electrochemical reduction of dications, the formation of biradicals via radical cation species was demonstrated by UV/Vis spectroscopy with several isosbestic points at both stages. Therefore, the cation-stacking approach is a promising way to provide novel properties due to perturbation of their molecular orbitals and to stabilize the reduced species even though they have open-shell characters.



https://doi.org/10.26434/chemrxiv-2024-fd9ws **ORCID:** https://orcid.org/0000-0001-7961-3595 Content not peer-reviewed by ChemRxiv. **License:** CC BY 4.0

## Introduction

Over the past few decades, many studies have been conducted on π-conjugated molecules, which have unique electronic properties based on an effective π-electron delocalization.[1,2] Since π-conjugated molecules with rigid and planar structures, in general, have p-orbitals overhanging perpendicular to the molecular plane, stacking of two or more molecular planes can affect the molecular orbitals themselves, leading to significant changes in physical properties such as absorption properties.[3,4] Therefore, when two π-conjugated units are close to a separation distance of 3.4 Å (the sum of van der Waals (vdW) radii of carbon atoms) or less by a stacked structure that can induce an interaction between their molecular orbitals by forming new orbitals through linear combination of the components, it is expected that they could exhibit unprecedented properties that are not seen with monomeric π-conjugated units. There have been several reports that the stacking of aromatic compounds can modify their intrinsic properties such as conductive/energy transfer properties[5,6] and absorption/emission properties due to the formation of H- or J-aggregates.[7,8] Recently, a unique property of three-dimensional (3D) aromaticity based on stacked anti-aromatic molecules has been reported by Shinokubo *et al* (Figure 1a).[9,10] A similar 3D (anti)aromaticity was also predicted by closely stacked aromatic units,[11–13] and thus the stacking of planar π-systems is key for the development of molecules with novel functions.

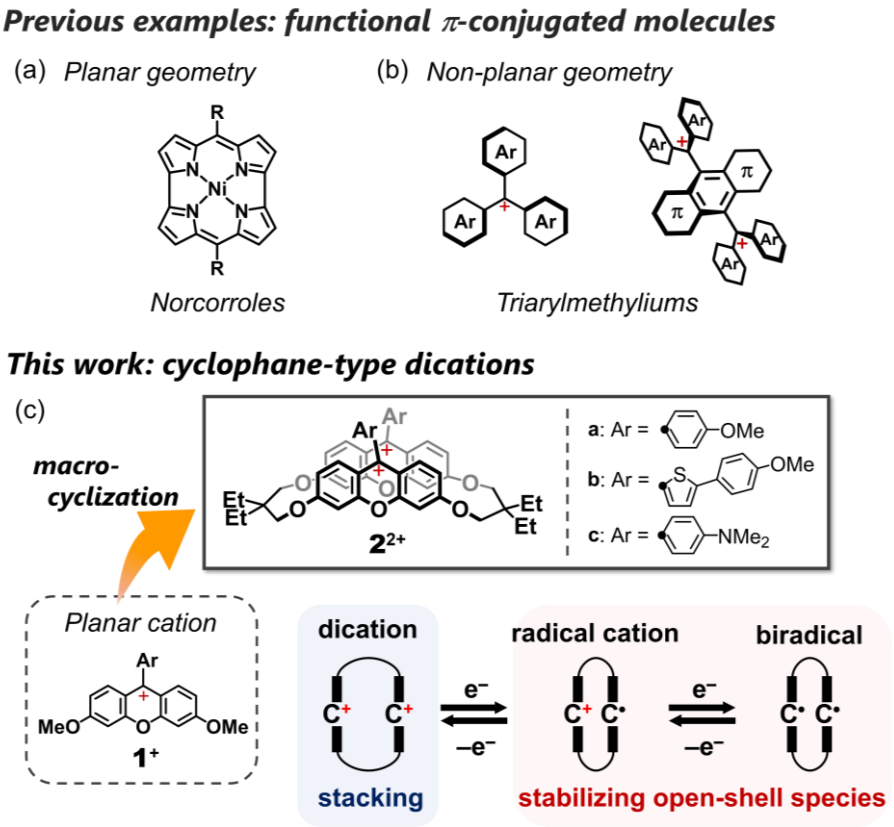


**Figure 1.** Previous examples: (a) norcorrole with a planar conjugated system exhibiting 3D-aromaticity by stacking of molecules and (b) redox-active cationic dyes with a propeller-like or twisted geometry, which is not suitable for stacking themselves. (c) This work: cyclophane-type dications with planar cationic units exhibiting stepwise redox interconversion thanks to the stabilization of reduced species by stacked structure.



https://doi.org/10.26434/chemrxiv-2024-fd9ws ORCID: https://orcid.org/0000-0001-7961-3595 Content not peer-reviewed by ChemRxiv. License: CC BY 4.0

Cationic π-conjugated molecules often exhibit a long-wavelength absorption with a large molar extinction coefficient due to the narrow HOMO-LUMO gap based on the effective delocalization of both charge and π-electrons.[14,15] In addition, since well-designed organic cations can interconvert with neutral species upon electron transfer (Figure 1b),[16–21] cationic π-conjugated molecules are promising candidates for functional organic materials such as chromic materials and organic semiconductors. When two or more cationic units can be stacked, they can show novel properties and functions, which can be switched by an external stimulus, such as an electric potential. However, under dispersed conditions, such as in solution, cation units cannot be stacked effectively to interact with each other, due to Coulombic repulsion and/or entropical disadvantage. Therefore, there are very few successful examples of realizing the proximity of cationic species,[22,23] when compared to the results with neutral molecules. Moreover, the redox behavior of stacked cations has not yet been well studied, and thus there is still room to explore novel properties of stacked multi-cationic species.

To date, three methods have been mainly used to construct stacked structures. First, by introducing functional groups and/or side chains into π-conjugated molecules with a wide π-plane, attractive interaction between molecules can induce aggregation, where the formation of aggregates is more enthalpically favorable in the crystalline state or under conditions of high concentration and low temperature.[24–26] Second, by the inclusion of two or more π-conjugated molecules in a cage-shaped molecule, molecules are forced to be stacked and interact with each other.[27] Third, by using cyclophane-type structures with two or more linkers, the π-planes are forced to be closely arranged and form a face-to-face stacked structure.[5,6,9,28–30]

Among them, we considered that cyclophane-type structures are suitable for realizing the stacking of cationic π-systems because the other two approaches would be less promising due to electrostatic repulsion between cationic units. We envisaged that, by stacking of the cationic units, considerable changes in color (e.g., blue- or red-shift) and reduction behavior (e.g., stepwise one-electron reduction) would be expected compared to the results with the corresponding monomeric cation. Thus, we designed cyclophane-type dications $\mathbf{2}^{2+}$ with coplanar xanthylium units, which would have a stacked geometry of reference monocations $\mathbf{1}^{+}$ (Figure 1c). In this study, we investigated the effect of the cyclophane-type structure on the physical properties and redox behavior of $\mathbf{2}^{2+}$. Due to the close proximity of cationic units realized by the above molecular design, the intramolecular interaction between cation units enables a change in absorption. Furthermore, this cation-stacking approach can stabilize their reduced species, allowing us to observe clean electrochromic behavior, even though the reduced states are open-shell species.

## Results and Discussion

### Molecular Design, Preparation, and X-ray Analysis

Based on the above concept, cyclophane-type dications $\mathbf{2}^{2+}$ with planar 3,6-dialkoxyxanthylium units were designed, with the expectation that the stacking of cationic units could be realized by effective interaction through three-carbon linkers. In addition, since reduction of $\mathbf{2}^{2+}$ efficiently decreases electrostatic repulsion between π-conjugated units to make further proximity between them, the redox interconversion with the one- or two-electron reduced species could allow reversible control of the


https://doi.org/10.26434/chemrxiv-2024-fd9ws ORCID: https://orcid.org/0000-0001-7961-3595 Content not peer-reviewed by ChemRxiv. License: CC BY 4.0

photophysical properties based on a change in the stacking environment (Figure 1d). Regarding the additional aryl group at the 9-position of xanthylium, 4-methoxyphenyl and 4-dimethylaminophenyl groups with different electron-donating properties were selected to investigate the influence of electronic properties. We also introduced a 5-(4-methoxyphenyl)-thienyl group, which is expected to stabilize radical cationic and biradical species based on the effective delocalization of a positive charge or an unpaired electron due to extension of the conjugated system.[18,31]

As shown in Scheme 1, cyclic diketone **7** was prepared by the reaction of 3,6-dihydroxyxanthen-9-one **4**[32] with tosylated 2,2-diethyl-1,3-propanediol **5**[33] in a stepwise manner. For the latter cyclic reaction, we adopted high dilution conditions (5 mM in DMF). The *gem*-diethyl-substituted linkers would contribute to the efficient formation (Thorpe-Ingold Effect[34]) of an intramolecular cyclic compound rather than linear oligomers, and the desired macrocyclic diketone **7** was isolated in 63% yield. When diketone **7** was reacted with the corresponding aryl lithium reagents, precursor diols **8a**−**8c** were obtained in 70%, 54%, and 73% yields, respectively.

For diols **8a**−**8c**, there could be several isomers for the arrangement of alcohols and/or the direction of xanthene units. The $^1$H NMR spectra in $CDCl_3$ revealed that **8a** and **8b** exist as single diastereomers; for the latter, X-ray analysis showed that **8b** adopts a *syn*-type geometry (Figure S18a). On the other hand, **8c** exists as a mixture of the two isomers (**8c-*syn*** and **8c-*anti***) according to $^1$H NMR spectroscopy and single-crystal X-ray analyses (Figure S18b,c). From the intensity of the $^1$H NMR signals, the ratio of the isomers for **8c** was estimated to be **8c-*syn***:**8c-*anti*** = 6:1. Both diastereomers of **8c** were used in the next reaction without further purification since a dehydration reaction would yield the same dication from both diastereomers. When **8a**−**8c** were subjected to dehydration under acidic conditions, the target cyclophane-type dication salts **2a**$^{2+}$$(BF_4^-)_2$−**2c**$^{2+}$$(BF_4^-)_2$ were successfully isolated as orange, wine red, and blue powders in 100%, 91%, and 92% yields, respectively.

**Scheme 1.** Synthesis of cyclophane-type dications **2a**$^{2+}$$(BF_4^-)_2$, **2b**$^{2+}$$(BF_4^-)_2$ and **2c**$^{2+}$$(BF_4^-)_2$.

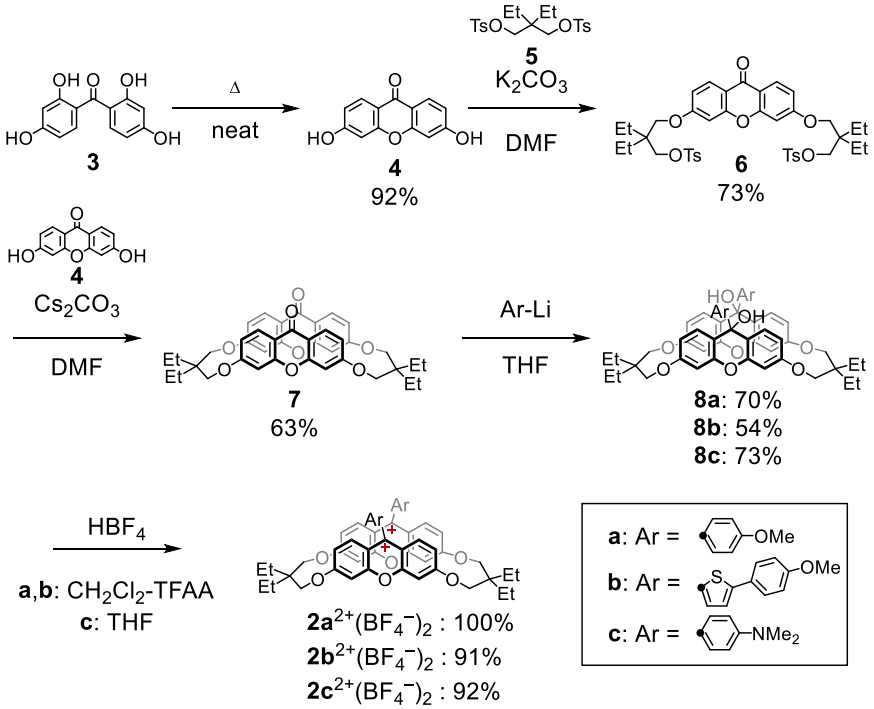




https://doi.org/10.26434/chemrxiv-2024-fd9ws **ORCID:** https://orcid.org/0000-0001-7961-3595 Content not peer-reviewed by ChemRxiv. **License:** CC BY 4.0

The reference compounds, monocation salts **1**$^{+}$$BF_4^{-}$, were prepared in a similar manner as for the synthesis of **2**$^{2+}$$(BF_4^{-})_2$ (Scheme S1). Monoketone **9** was prepared by the reaction of 3,6-dihydroxyxanthen-9-one **4** with iodomethane under basic conditions. When monoketone **9** was reacted with the corresponding aryl lithium reagents, precursor alcohols **10a**−**10c** were obtained in 92%, 80%, and 77% yields, respectively. When **10a**−**10c** were treated with acid, the reference monocation salts **1a**$^{+}$$BF_4^{-}$−**1c**$^{+}$$BF_4^{-}$ were obtained as orange, wine red, and blue powders in 96%, 93%, and 97% yields, respectively.

X-ray analyses of **2a**$^{2+}$$(BF_4^{-})_2$ and **1a**$^{+}$$BF_4^{-}$ using a single crystal obtained by recrystallization from $CH_2Cl_2$/$Et_2O$ revealed that there are the shortest intermolecular C···C contacts of 3.3799(19) Å for **1a**$^{+}$$BF_4^{-}$ and 3.189(5) Å for **2a**$^{2+}$$(BF_4^{-})_2$, respectively, both of which are smaller than the sum of the vdW radii of carbon atoms (3.4 Å)[35] (Figure 2). The value for **2a**$^{2+}$ is smaller than that for **1a**$^{+}$. Therefore, obvious intramolecular interactions due to π-π stacking between cation units were expected for the cyclophane-type dications. Another feature of the packing structure is that, in cyclophane-type dication salt **2a**$^{2+}$$(BF_4^{-})_2$, two chromophores in the crystal are facing each other and stacked in a parallel manner, unlike that of monocation salt **1a**$^{+}$$BF_4^{-}$ (Figure 2-2). Compared to the dihedral angle $\theta$[11.15(6)°] between the triarylmethyl moieties for **1a**$^{+}$$BF_4^{-}$, the smaller value [7.71(19)°] was observed for **2a**$^{2+}$$(BF_4^{-})_2$, i.e., cation units are almost overlapped in parallel thanks to the cyclophane structure. These results show that the molecular design of the introduction of the highly planar π-system is effective for stacking of the cationic units.

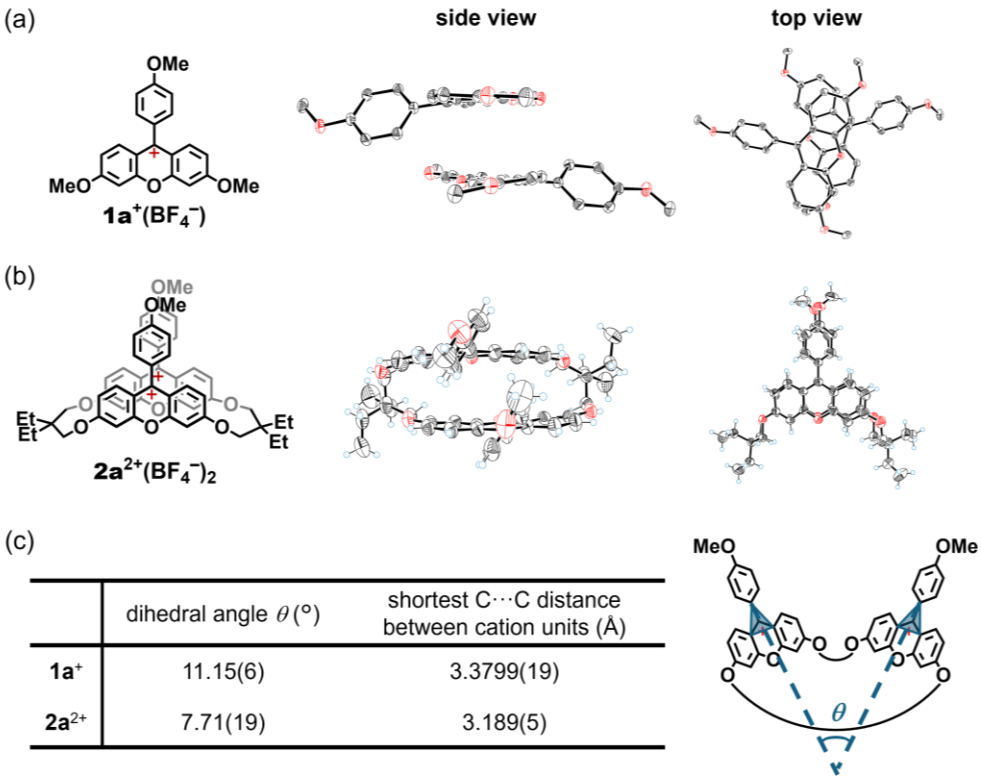


| | dihedral angle $\theta$ (°) | shortest C···C distance between cation units (Å) |
|---|---|---|
| **1a**$^{+}$ | 11.15(6) | 3.3799(19) |
| **2a**$^{2+}$ | 7.71(19) | 3.189(5) |

**Figure 2.** ORTEP drawings of (a) **1a**$^{+}$$BF_4^{-}$ and (b) **2a**$^{2+}$$(BF_4^{-})_2$. Thermal ellipsoids are shown at the 50% probability level. Counterions and solvent molecules are omitted for clarity. (c) The dihedral angle $\theta$ and the shortest C···C distance between cation units of **1a**$^{+}$$BF_4^{-}$ and **2a**$^{2+}$$(BF_4^{-})_2$.


https://doi.org/10.26434/chemrxiv-2024-fd9ws **ORCID:** https://orcid.org/0000-0001-7961-3595 Content not peer-reviewed by ChemRxiv. **License:** CC BY 4.0

## UV/Vis Spectroscopy and Theoretical Investigation

UV/Vis spectra of the $BF_4^-$ salts of dications and monocations were measured in $CH_2Cl_2$ (Figure 3). All macrocyclic dications exhibit strong absorptions in the visible region [$\lambda_{max}$/nm (log $\varepsilon$): 420 (5.00) for **2a**$^{2+}(BF_4^-)_2$, 561 (4.48), 434 (4.79) for **2b**$^{2+}(BF_4^-)_2$, and 603 (4.68), 414 (4.92) for **2c**$^{2+}(BF_4^-)_2$, respectively]. Compared to reference monocations [$\lambda_{max}$ / nm (log $\varepsilon$): 439 (4.82) for **1a**$^+BF_4^-$, 561 (4.29), 446 (4.70) for **1b**$^+BF_4^-$, and 606 (4.39), 425 (4.70) for **1c**$^+BF_4^-$, respectively], a blue shift and an increase in full width at half-maximum (FWHM) of the absorption band at around 420 nm were observed for cyclophane-type dications **2**$^{2+}$ (Figure 3). This means that there is a contribution from H-type aggregates,[7,8] and thus, even in solution, cation units in dication **2**$^{2+}$ have a stacking geometry similar to those in the single crystal. Furthermore, the absorption maxima of the first band for these cations drastically changes depending on the donating ability of the substituent on the aryl group due to the significant change in the HOMO level.

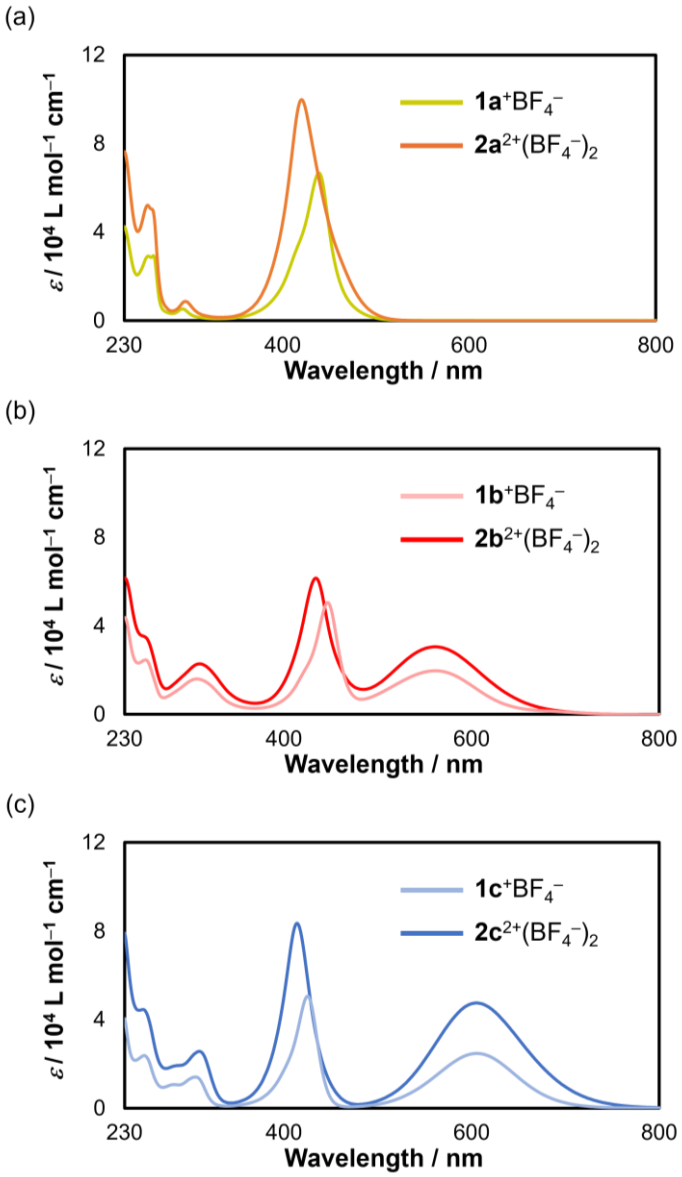


**Figure 3.** UV/Vis spectra of (a) **1a**$^+BF_4^-$ (28.3 μM, yellow) and **2a**$^{2+}(BF_4^-)_2$ (12.4 μM, orange), (b) **1b**$^+BF_4^-$ (24.2 μM, pink) and **2b**$^{2+}(BF_4^-)_2$ (14.1 μM, red), and (c) **1c**$^+BF_4^-$ (28.8 μM, light blue) and **2c**$^{2+}(BF_4^-)_2$ (13.0 μM, blue) in $CH_2Cl_2$.



https://doi.org/10.26434/chemrxiv-2024-fd9ws **ORCID:** https://orcid.org/0000-0001-7961-3595 Content not peer-reviewed by ChemRxiv. **License:** CC BY 4.0

To gain insight into the stabilization energy by the stacking of cation units for cyclophane-type dications **2**$^{2+}$, the relative energies among the conformers was investigated using DFT calculations at the $\omega$B97X-D/6-31G* level. As shown in Figures 4a and S19-S21, the relative energies for the semi-open form and the open form are much higher than that for the closed form with the stacked geometry, which is calculated to be the most stable structure for all dications (semi-open form: $\Delta E_{rel}$ = 6.79 kcal mol$^{-1}$ for **2a**$^{2+}$, 15.11 kcal mol$^{-1}$ for **2b**$^{2+}$, and 6.68 kcal mol$^{-1}$ for **2c**$^{2+}$ and open form: $\Delta E_{rel}$ = 19.55 kcal mol$^{-1}$ for **2a**$^{2+}$, 20.68 kcal mol$^{-1}$ for **2b**$^{2+}$, and 18.77 kcal mol$^{-1}$ for **2c**$^{2+}$). This result indicates that the stacking of cationic units has a stabilization effect, which is greater than the electrostatic repulsion. Indeed, the noncovalent interaction (NCI) plots[36] of **2**$^{2+}$ at the $\omega$B97X-D/6-31G* level show that, due to the delocalization of a positive charge that efficiently reduces electrostatic repulsion, the cation units facing each other of **2**$^{2+}$ exert attractive rather than repulsive effects (Figures 4b and S34).

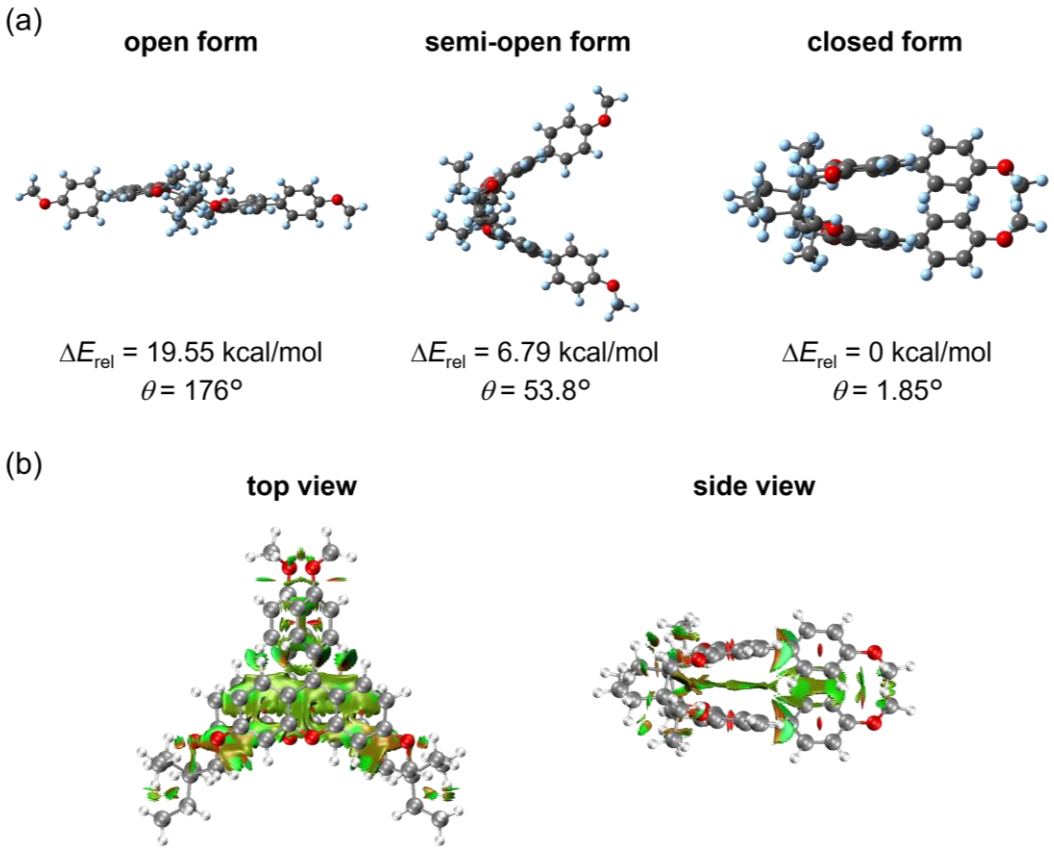


**Figure 4.** (a) Optimized structures and (b) NCI plots [isovalue= 0.5 a.u., front and side views] of **2a**$^{2+}$ obtained by DFT calculations at the $\omega$B97X-D/6-31G* level of theory. Color online: blue, strong attractive interactions; green, vdW interactions; red, repulsive/steric interactions.

### Reversible Redox Behavior Realized by a Cyclophane-type Structure

To investigate the redox properties in detail, cyclic voltammetry was carried out in $CH_2Cl_2$ with ferrocene as an external standard (Figure 5). For all dications **2**$^{2+}$, the voltammograms showed two-stage one-electron (1e)-reduction waves ($E_1^{red}$ and $E_2^{red}$/V vs. SCE: −0.15, −0.32 for **2a**$^{2+}$, −0.05, −0.23 for **2b**$^{2+}$, and −0.25, −0.43 for **2c**$^{2+}$). Considering that cation units must undergo simultaneous two-electron (2e)-reduction at a potential similar to that of monocations **1**$^{+}$ ($E_1^{red}$/V vs. SCE: −0.25 for **1a**$^{+}$, −0.15 for **1b**$^{+}$,


https://doi.org/10.26434/chemrxiv-2024-fd9ws ORCID: https://orcid.org/0000-0001-7961-3595 Content not peer-reviewed by ChemRxiv. License: CC BY 4.0

and −0.34 for **1c**$^{+}$) when there is no interaction between the cation units,[37] the stepwise reduction processes indicate that the cation units are close enough to interact with each other even in solution. In addition, unlike with monocations **1**$^{+}$ which exhibit an irreversible process, reversible redox waves were observed for dications **2**$^{2+}$, indicating that the cyclophane structure can stabilize both radical cation and biradical species. Although the closed-shell species might be obtained by the bond formation between the two radicals upon the 2e-reduction of **2**$^{2+}$, the reversible waves show that the σ-bond was not formed. Such species with a σ-bond should have a much lower HOMO level, leading to an anodic shift of the oxidation potential,[16] however, it is not the case. DFT calculations also suggest that the most stable structure is the open-shell species **2**$^{\bullet\bullet}$, and thus, the σ-bonded species can be excluded in the later discussion. The differences in reduction potentials among the three dications **2**$^{2+}$ with different substituents are small (~0.2 V) for both $E_1^{red}$ and $E_2^{red}$/V, suggesting that the coefficients of LUMO of **2**$^{2+}$ are mainly located on the xanthylium units. Furthermore, a twisted geometry of the aryl group to the xanthylium unit also suppresses effective conjugation. Thus, the donating ability of aryl groups does not affect the reduction potentials.

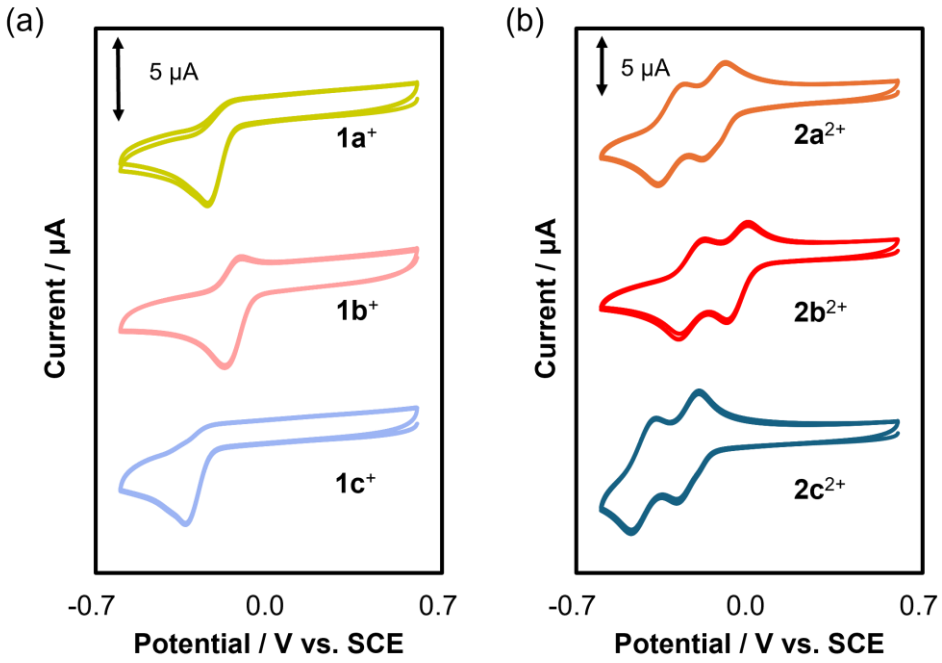


**Figure 5.** Cyclic voltammograms of (a) **1a**$^{+}BF_4^{-}$, **1b**$^{+}BF_4^{-}$, and **1c**$^{+}BF_4^{-}$ and (b) **2a**$^{2+}(BF_4^{-})_2$, **2b**$^{2+}(BF_4^{-})_2$, and **2c**$^{2+}(BF_4^{-})_2$ in $CH_2Cl_2$ containing 0.1 M $Bu_4NBF_4$ as a supporting electrolyte (scan rate 100 $mVs^{-1}$, Pt electrode).



https://doi.org/10.26434/chemrxiv-2024-fd9ws **ORCID:** https://orcid.org/0000-0001-7961-3595 Content not peer-reviewed by ChemRxiv. **License:** CC BY 4.0

**Table 1.** UV/Vis spectral data and the reduction potentials of the $BF_4^-$ salts in $CH_2Cl_2$.

| UV/Vis | $\lambda_{max}$/nm (FWHM/nm) | Redox behavior | $E_1^{red}$/V | $E_2^{red}$/V |
|---|---|---|---|---|
| **2a**$^{2+}$ | 420 [44] | **2a**$^{2+}$/**2a**$^{\bullet+}$/**2a**$^{\bullet\bullet}$ | -0.15 | -0.32 |
| **2b**$^{2+}$ | 561 [112]<br>434 [37] | **2b**$^{2+}$/**2b**$^{\bullet+}$/**2b**$^{\bullet\bullet}$ | -0.05 | -0.23 |
| **2c**$^{2+}$ | 603 [111]<br>414 [34] | **2c**$^{2+}$/**2c**$^{\bullet+}$/**2c**$^{\bullet\bullet}$ | -0.25 | -0.43 |
| **1a**$^{+}$ | 439 [36] | **1a**$^{+}$/**1a**$^{\bullet}$ | $E_{pc}$[a] = -0.25 V | |
| **1b**$^{+}$ | 561 [107]<br>446 [30] [ | **1b**$^{+}$/**1b**$^{\bullet}$ | $E_{pc}$[a] = -0.15 V | |
| **1c**$^{+}$ | 606 [99]<br>425 [29] | **1c**$^{+}$/**1c**$^{\bullet}$ | $E_{pc}$[a] = -0.34 V | |

[a] Peak potential is shown as $E_{pc}$ (V vs. SCE).

**Electrochromic Behavior and Redox Interconversion**

Based on the voltammetric studies, we considered that we could observe radical cation and biradical species as long-lived species in spectroelectrograms, thanks to stabilization by the cyclophane structure. Upon constant-potential electrochemical reduction in $CH_2Cl_2$ for **2a**$^{2+}$$(BF_4^-)_2$, biradical species was successfully observed via radical cation under the application of a voltage from +0.50 to −0.25 V vs. SCE [$\lambda_{max}$/nm: 429, 447 for **2a**$^{\bullet+}$ at −0.25 V; 451 for **2a**$^{\bullet\bullet}$ at −0.70 V] (Figure 6b). There are several isosbestic points in both steps (273 nm for the first step and 293 nm for the second step). These absorption bands for the reduced species by UV/Vis spectroscopy are in good agreement with those by TD-DFT calculations (Figure 6c-f). Similar behaviors were successfully observed upon constant-potential electrochemical reduction for **2b**$^{2+}$$(BF_4^-)_2$ and **2c**$^{2+}$$(BF_4^-)_2$ [$\lambda_{max}$/nm: 438, 562 for **2b**$^{\bullet+}$ at −0.15 V; 456, 559 for **2b**$^{\bullet\bullet}$ at −0.60 V; 420, 606 for **2c**$^{\bullet+}$ at −0.35 V; 425, 604 for **2c**$^{\bullet\bullet}$ at −0.70 V] (Figure S38).

In addition, continuous electrochromic behavior was demonstrated upon constant-current electrochemical reduction and subsequent oxidation in $CH_2Cl_2$ for **2**$^{2+}$$(BF_4^-)_2$, which was monitored by UV/Vis spectroscopy. For **2a**$^{2+}$$(BF_4^-)_2$ and **2b**$^{2+}$$(BF_4^-)_2$, clean electrochromism was observed via radical cation species in both redox processes, and the original spectra were regenerated by electrochemical oxidation of as-prepared biradical species (Figures S39 and S40). Clean electrochromic behavior is noteworthy even when it is realized by involving the biradical state. Therefore, the stacked geometry can certainly stabilize radical cation and biradical species, due to the effective interaction between planar π-units, as found in the dications.

To isolate the biradical species and confirm the reversibility of redox interconversion, chemical reduction and subsequent oxidation of **2**$^{2+}$$(BF_4^-)_2$ were performed. As shown in Scheme 2, upon two-electron reduction of cyclophane-type dicationic salts **2a**$^{2+}$$(BF_4^-)_2$, **2b**$^{2+}$$(BF_4^-)_2$, and **2c**$^{2+}$$(BF_4^-)_2$ with two equivalents of cobaltocene in dry MeCN, biradical species **2a**$^{\bullet\bullet}$, **2b**$^{\bullet\bullet}$ and **2c**$^{\bullet\bullet}$ were isolated in 63%, 97%, and 89% yields as yellow, brown, and green solids, respectively. We also confirmed that the UV/Vis


https://doi.org/10.26434/chemrxiv-2024-fd9ws **ORCID:** https://orcid.org/0000-0001-7961-3595 Content not peer-reviewed by ChemRxiv. **License:** CC BY 4.0

spectra of isolated **2**•• are in good agreement with those of as-prepared **2**•• upon electrochemical reduction. In addition, upon treatment of biradical species **2a**••, **2b**••, and **2c**•• with two equivalents of (4-$BrC_6H_4)_3N^{+\bullet}BF_4^-$ in dry $CH_2Cl_2$, dicationic salts $\mathbf{2a}^{2+}(BF_4^-)_2$, $\mathbf{2b}^{2+}(BF_4^-)_2$ and $\mathbf{2c}^{2+}(BF_4^-)_2$ were recovered in 100%, 100% and 87% yields, respectively. Reversible redox interconversion was demonstrated in all cases, because biradical species can be handled as a stable entity thanks to the cyclophane structure.

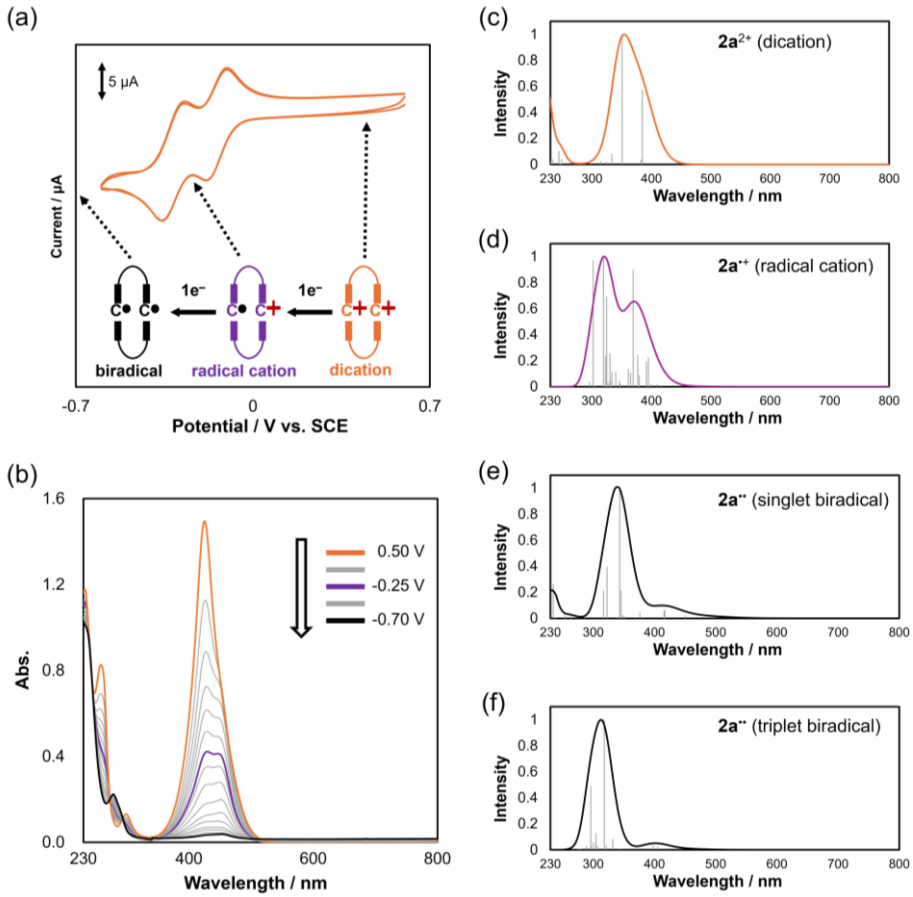


**Figure 6.** (a) Redox scheme of $\mathbf{2a}^{2+}$ with cyclic voltammogram, which was measured in $CH_2Cl_2$ containing 0.1 M $Bu_4NBF_4$ as a supporting electrolyte (scan rate 100 $mVs^{-1}$, Pt electrode). (b) Changes in the UV-Vis spectrum of $\mathbf{2a}^{2+}(BF_4^-)_2$ (150 μM) upon constant-potential electrochemical reduction to **2a**•• via $\mathbf{2a}^{\bullet+}$ in $CH_2Cl_2$ containing 0.1 M $Bu_4NBF_4$ as a supporting electrolyte. Simulated UV/Vis spectra for (c) $\mathbf{2a}^{2+}$, (d) $\mathbf{2a}^{\bullet+}$, (e) **2a**•• (singlet state), and (f) **2a**•• (triplet state) by TD-DFT calculations at the (U)ωB97X-D/6-31G* level.

**Scheme 2.** Redox interconversion between $\mathbf{2}^{2+}(BF_4^-)_2$ and **2**••.

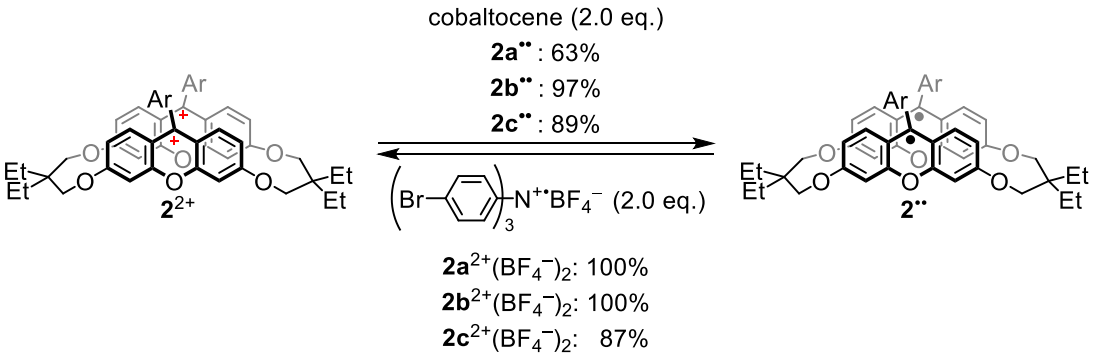




https://doi.org/10.26434/chemrxiv-2024-fd9ws **ORCID:** https://orcid.org/0000-0001-7961-3595 Content not peer-reviewed by ChemRxiv. **License:** CC BY 4.0

When the $^1$H NMR measurements of the isolated neutral species **2** were conducted in $CDCl_3$ (Figures S15-17), slight broad signals in the aliphatic region were observed while the aromatic region was nearly silent. These results indicate that the reduced species obtained by chemical reduction of $\mathbf{2}^{2+}(BF_4^-)_2$ have an open-shell character (e.g., thermally excited triplet state of biradicals). Next, electron spin resonance (ESR) measurements of the biradical species $\mathbf{2}^{\bullet\bullet}$ were performed in toluene (Figure S42). Very weak signals assignable to the species with open-shell characters were observed, indicating that the singlet state is more stable for these biradicals. Therefore, for $\mathbf{2}^{\bullet\bullet}$, although there is a marginal contribution from the thermally excited triplet species in solution, the singlet state can be stabilized by a spin-spin interaction in the cyclophane-type structure. This study demonstrates that the cyclophane structure composed of planar π-conjugated cations is an effective way not only to modulate physical properties such as absorption and redox properties but also to stabilize the corresponding reduced species including a biradical state.

## Conclusion

In conclusion, we designed and synthesized cyclophane-type dications $\mathbf{2a}^{2+}$–$\mathbf{2c}^{2+}$, composed of two units of planar π-units xanthylium $\mathbf{1}^+$ with the alkylene linkers. X-ray analyses of dication salts $\mathbf{2a}^{2+}(BF_4^-)_2$–$\mathbf{2c}^{2+}(BF_4^-)_2$ showed that the cation units are closely stacked and facing each other in the crystal due to the non-covalent interaction between planar π-units, which was demonstrated by NCI plots. Cyclic voltammetry and UV/Vis spectroscopy revealed that there is an intramolecular interaction between the cation units of $\mathbf{2a}^{2+}(BF_4^-)_2$–$\mathbf{2c}^{2+}(BF_4^-)_2$ by stacking in parallel (H-type aggregates) even in solution. Furthermore, by modifying the electron-donating ability of the substituent on the aryl group, the color tone of the dications can be modulated without changing the LUMO level. Such a stacking structure observed in $\mathbf{2}^{2+}$ can also stabilize their radical cation and biradical species, and thus cyclophane-type dications $\mathbf{2}^{2+}$ exhibit clean electrochromic behavior via an intermediary radical cation and biradical. In addition, biradical species $\mathbf{2a}^{\bullet\bullet}$–$\mathbf{2c}^{\bullet\bullet}$ were successfully isolated upon two-electron reduction of cyclophane-type dicationic salts $\mathbf{2a}^{2+}(BF_4^-)_2$–$\mathbf{2c}^{2+}(BF_4^-)_2$. Therefore, the cation-stacking approach can be a versatile method for developing stimuli-responsive molecules and stabilizing intrinsically unstable open-shell species.


## Acknowledgements

This work was supported by Grant-in-Aid from MEXT and JSPS (Nos. JP23K20275 to T.S. and JP23K21107 and JP23H04011 to Y.I.). Y.I. acknowledges JST PRESTO (No. JPMJPR23Q1). This work was also supported by the “Five-star Alliance” in “NJRC Mater. & Dev.” MEXT.

**Keywords:** Cations • Cyclophane • Electrochromism • Radicals • Redox systems


## References


[1] R. E. Martin, F. Diederich, *Angew. Chem. Int. Ed.* **1999**, *38*, 1350–1377.

[2] H. Meier, *Angew. Chem. Int. Ed.* **2005**, *44*, 2482–2506.

[3] F. J. M. Hoeben, P. Jonkheijm, E. W. Meijer, A. P. H. J. Schenning, *Chem. Rev.* **2005**, *105*, 1491–1546.




https://doi.org/10.26434/chemrxiv-2024-fd9ws **ORCID:** https://orcid.org/0000-0001-7961-3595 Content not peer-reviewed by ChemRxiv. **License:** CC BY 4.0

[4] Z. Chen, A. Lohr, C. R. Saha-Möller, F. Würthner, *Chem. Soc. Rev.* **2009**, *38*, 564–584.
[5] K. Bechgaard, K. Carneiro, F. B. Rasmussen, M. Olsen, G. Rindorf, C. S. Jacobsen, H. J. Pedersen, J. C. Scott, *J. Am. Chem. Soc.* **1981**, *103*, 2440–2442.
[6] Y. Morisaki, N. Kawakami, S. Shibata, Y. Chujo, *Chem. – An Asian J.* **2014**, *9*, 2891–2895.
[7] M. Kasha, *Radiat. Res.* **1963**, *20*, 55–70.
[8] N. J. Hestand, F. C. Spano, *Chem. Rev.* **2018**, *118*, 7069–7163.
[9] R. Nozawa, J. Kim, J. Oh, A. Lamping, Y. Wang, S. Shimizu, I. Hisaki, T. Kowalczyk, H. Fliegl, D. Kim, H. Shinokubo, *Nat. Commun.* **2019**, *10*, 3576.
[10] S. Kino, S. Ukai, N. Fukui, R. Haruki, R. Kumai, Q. Wang, S. Horike, Q. M. Phung, D. Sundholm, H. Shinokubo, *J. Am. Chem. Soc.* **2024**, *146*, 9311–9317.
[11] M. C. Böhm, P. Bickert, K. Hafner, V. Boekelheide, *Proc. Natl. Acad. Sci.* **1984**, *81*, 2589–2591.
[12] T. Nishiuchi, Y. Makihara, R. Kishi, H. Sato, T. Kubo, *J. Phys. Org. Chem.* **2023**, *36*, e4451.
[13] Y. Tsuji, K. Okazawa, K. Yoshizawa, *J. Org. Chem.* **2023**, *88*, 14887–14898.
[14] D. F. Duxbury, *Chem. Rev.* **1993**, *93*, 381–433.
[15] J. Bosson, J. Gouin, J. Lacour, *Chem. Soc. Rev.* **2014**, *43*, 2824–2840.
[16] T. Nishinaga, *Organic Redox Systems*, John Wiley & Sons, Inc, Hoboken, NJ, **2015**.
[17] T. Harimoto, Y. Ishigaki, *ChemPlusChem* **2022**, *87*, e202200013.
[18] Y. Ishigaki, T. Hashimoto, K. Sugawara, S. Suzuki, T. Suzuki, *Angew. Chem. Int. Ed.* **2020**, *59*, 6581–6584.
[19] M. B. S. Wonink, B. P. Corbet, A. A. Kulago, G. B. Boursalian, B. de Bruin, E. Otten, W. R. Browne, B. L. Feringa, *J. Am. Chem. Soc.* **2021**, *143*, 18020–18028.
[20] K. Li, Z. Xu, J. Xu, T. Weng, X. Chen, S. Sato, J. Wu, Z. Sun, *J. Am. Chem. Soc.* **2021**, *143*, 20419–20430.
[21] T. Nishiuchi, K. Uchida, T. Kubo, *Chem. Commun.* **2023**, *59*, 7379–7382.
[22] A. J. Wallace, C. D. Jayasinghe, M. I. J. Polson, O. J. Curnow, D. L. Crittenden, *J. Am. Chem. Soc.* **2015**, *137*, 15528–15532.
[23] M. Murai, M. Abe, S. Ogi, S. Yamaguchi, *J. Am. Chem. Soc.* **2022**, *144*, 20385–20393.
[24] Y. Arai, H. Segawa, *J. Phys. Chem. B* **2011**, *115*, 7773–7780.
[25] F. Fennel, S. Wolter, Z. Xie, P.-A. Plötz, O. Kühn, F. Würthner, S. Lochbrunner, *J. Am. Chem. Soc.* **2013**, *135*, 18722–18725.
[26] X. Tang, L. Tu, X. Zhao, J. Chen, Y. Ning, F. Wu, Z. Xiong, *J. Phys. Chem. C* **2022**, *126*, 9456–9465.
[27] J. K. Klosterman, Y. Yamauchi, M. Fujita, *Chem. Soc. Rev.* **2009**, *38*, 1714–1725.
[28] F. N. Diederich, *Cyclophanes*, The Royal Society Of Chemistry, **1991**.
[29] R. Gleiter, H. Hopf, Eds. , *Modern Cyclophane Chemistry*, Wiley, **2004**.
[30] P. G. Ghasemabadi, T. Yao, G. J. Bodwell, *Chem. Soc. Rev.* **2015**, *44*, 6494–6518.
[31] S.-G. Chong, S. Suzuki, T. Suzuki, Y. Ishigaki, *Bull. Chem. Soc. Jpn.* **2023**, *96*, 1144–1149.
[32] L. A. Andronico, A. Quintavalla, M. Lombardo, M. Mirasoli, M. Guardigli, C. Trombini, A. Roda, *Chem. – A Eur. J.* **2016**, *22*, 18156–18168.
[33] E. R. Nelson, M. Maienthal, L. A. Lane, A. A. Benderly, *J. Am. Chem. Soc.* **1957**, *79*, 3467–3469.
[34] M. E. Jung, G. Piizzi, *Chem. Rev.* **2005**, *105*, 1735–1766.
[35] A. Bondi, *J. Phys. Chem.* **1964**, *68*, 441–451.
[36] J. Contreras-García, E. R. Johnson, S. Keinan, R. Chaudret, J.-P. Piquemal, D. N. Beratan, W. Yang, *J. Chem. Theory Comput.* **2011**, *7*, 625–632.
[37] Y. Ishigaki, T. Tachibana, K. Sugawara, M. Kikuchi, T. Suzuki, *ChemPlusChem* **2023**, *88*, e202300110.
[38] CCDC numbers: 2349747-2349755.


https://doi.org/10.26434/chemrxiv-2024-fd9ws **ORCID:** https://orcid.org/0000-0001-7961-3595 Content not peer-reviewed by ChemRxiv. **License:** CC BY 4.0